

Characterization of Temperature-Dependent Iron–Imidazole Vibrational Modes in Far Infrared

Sabine Dörr,[†] Ulrich Schade,[‡] Petra Hellwig,^{*,†} and Michele Ortolani[‡]

Laboratoire de spectroscopie vibrationnelle et électrochimie des biomolécules, Institut de Chimie, UMR 7177, Université Louis Pasteur, 4 rue Blaise Pascal, F-67000 Strasbourg, France, and Berliner Elektronenspeicherring-Gesellschaft für Synchrotronstrahlung mbH, Albert-Einstein-Strasse 15, D-12489 Berlin, Germany

Received: August 19, 2007; In Final Form: October 22, 2007

The active site of several oxygen binding proteins can be mimicked with the ferric iron protoporphyrin IX derivative hemin, coordinating two imidazole molecules and embedded in sodium dodecyl sulfate (SDS) micelles; the detergent simulates the hydrophobic cavity of heme proteins. We studied the low-frequency vibrational modes of the porphyrin–iron–imidazole bonding in infrared absorbance spectra. Assignment of the metal–ligand vibrations to signals at 396, 387, and 378 cm^{-1} was performed by isotope labeling of the imidazole ligand. These modes were also found to be temperature-dependent and to display a linear increase of signal intensity between 25 and 150 K and, with a different slope, between 150 and 300 K. The modes at 396 and 399 cm^{-1} show for 25 K an upshift about 4 cm^{-1} and the signal at 378 cm^{-1} a small downshift, indicating the involvement of antisymmetric stretching modes and, in the latter, of bending motions. Anharmonic couplings to doming modes are discussed, and the doming mode and hydrogen-bonding signature spectral range between 300 and 100 cm^{-1} is presented.

Introduction

The iron–histidine bond in heme proteins, such as hemoglobin, myoglobin, and cytochrome *c* oxidase, is the only covalent bond between protein and the active site where oxygen binds.^{6,7} It is affected by changes in protein structure and dynamics. Therefore it is of high interest in biochemistry and molecular biophysics.

Histidine is one of the α -amino acids and it is commonly found as a ligand to the metal ions in metalloenzymes.^{1–5} The infrared vibrational modes of histidine were previously investigated by density functional theory (DFT) calculations^{8,9} as well as measurements of model compounds,^{10–15} like imidazole or poly-L-histidine, and measurements of histidine in proteins, such as photosystem II and complexes of the respiratory chain.^{16–22} Mostly stretching vibrations of the imidazole ring were of interest, especially the C–N ring vibration at 1100 cm^{-1} and the NH_3^+ vibration at 1630 cm^{-1} . Signals due to the ligation of the metal centers in porphyrins are expected in the far-infrared, and would be of great interest for the understanding of metal–ligand vibrations in proteins, but they have been studied very little.²³

With the help of resonance Raman spectroscopy, however, these features were studied in great detail, including a significant signal between 250 and 200 cm^{-1} , the $\nu(\text{Fe–His})$ vibration.^{24–28} The position and intensity of this band essentially depends on the protein's nature, conformation, and the type of environment. This signal was studied both in proteins and in model complexes, like $\text{Fe}(\text{P})(\text{Im})$.^{29–34} Temperature-dependent measurements indicate that the band shifts to higher wavenumbers upon cooling.^{35–37} No corresponding analysis in far-infrared is available.

At lower frequencies a broad signal is seen in infrared that is discussed to include coordinates from doming modes and of hydrogen-bonding signatures. These modes show pronounced temperature dependence, previously reported for water. In order to differentiate the effects of the solvent or protein moiety and the metal-containing site, a clear analysis is necessary. For water, a number of temperature-dependent studies with infrared spectroscopy are available as well as theoretical approaches.^{38–40}

The approach presented here investigate the temperature dependence of the heme model compound hemin^{41,42} in SDS micelles with imidazole and isotopic labeled imidazole-*d*₄ as dried films on silicon wafers in the spectral region from 650 to 50 cm^{-1} . We could observe the vibrational features of the iron ligand OH and imidazole and the behavior of the hydrogen bonding upon cooling (300 to 25 K). The temperature-dependent behavior of the iron ligand vibrations and the hydrogen-bonding spectral region upon cooling are presented. Assignments are supported by isotope labeling of the imidazole ligand.

Materials and Methods

The samples were purchased from Sigma–Aldrich [hemin, imidazole, sodium dodecyl sulfate (SDS)] and ICON Isotopes (imidazole-*d*₄) and were used without further purification. Hemin was solved in aqueous NaOH solution pH 13–14 and a 10% solution of sodium dodecyl sulfate (SDS) with a final concentration of 1 mM.

The ferric bis(imidazolate) derivative was prepared by adding an excess of solid imidazole/imidazole-*d*₄ to the hemin solution. Different concentrations were used with a best result for 1 mM hemin and a higher concentration of imidazole. Control of the ligand binding was performed in the visible range and the typical shift of the α -band at 600 nm was monitored (data not shown). The absorbance spectra were obtained from thin films on silicon

* Corresponding author: e-mail hellwig@chimie.u-strasbg.fr.

[†] Université Louis Pasteur.

[‡] Berliner Elektronenspeicherring-Gesellschaft für Synchrotronstrahlung.

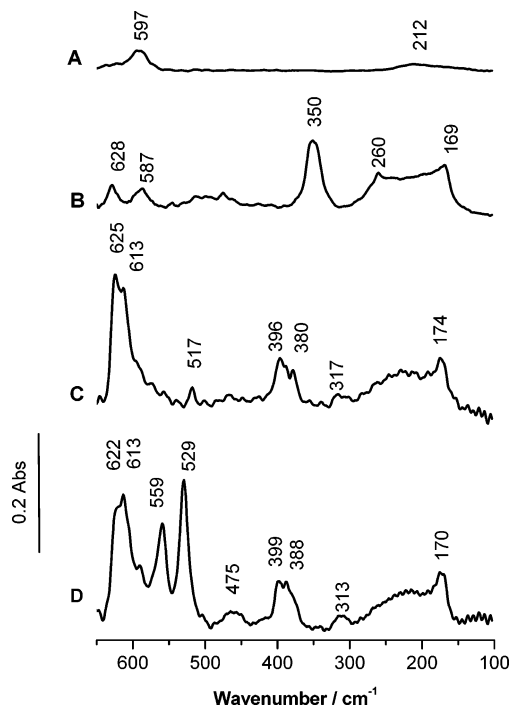


Figure 1. Absorbance spectra of (A) SDS, (B) hemin, (C) hemin with imidazole, and (D) hemin with imidazole- d_4 between 650 and 100 cm^{-1} at room temperature.

wafers with a Bruker IFS 66 Fourier transform infrared (FTIR) spectrometer. For far-infrared measurements, the instrument was equipped with an Hg source and detection was performed with a silicon bolometer (Infrared Labs). A 6 μm Mylar beam splitter was used. Two times 128 scans with a resolution of 2 cm^{-1} were averaged for each temperature step at a velocity of 40 kHz. The temperature-dependent measurements from 300 to 25 K were made with a helium-cooled cryostat (Janis Research).

Results and Discussion

Far-Infrared Spectroscopic Features of Bis(imidazole)–Iron Protoporphyrin. As a model for Fe–N ligation, which is the only covalent linkage in several proteins, a ferric iron protoporphyrin IX derivative (hemin), was investigated in the presence of detergent, namely, sodium dodecyl sulfate (SDS). The detergent simulates the hydrophobic cavity of hemoproteins. The chloride ligand, typically found in hemin, is exchanged to OH.³² After addition of solid imidazole, bis(imidazole)–iron protoporphyrin is formed. The ligand exchanges were followed by UV/vis spectroscopy (data not shown).

Figure 1 displays the infrared absorbance spectra of (A) SDS and (B) hemin in the presence of SDS in NaOH solution, as well as hemin with (C) imidazole and (D) imidazole- d_4 under the same conditions for the spectral region from 650 to 100 cm^{-1} . In the spectrum of the pure detergent, SDS, the signal of the C–S vibrational signal is found at 597 cm^{-1} and that of coupled CH vibrations is at 212 cm^{-1} . On this basis, the contributions of SDS in Figure 1B–D can be depicted.

Hemin shows two peaks at 260 and 169 cm^{-1} . The signal seen at 169 cm^{-1} is also found in the data of hemin with imidazole/imidazole- d_4 (174/170 cm^{-1}) and is thus not sensitive to the ligation state of the Fe center. In curves B–D in Figure 1, a broad feature between 300 and 150 cm^{-1} can be observed. The broadness and shape of this signal is not similar. It can be assigned as the contributions due to the so-called hydrogen-bonding signature,^{40,43} which is expected in this spectral region but also includes so-called doming modes.⁴⁴

The signals between 650 and 500 cm^{-1} include mainly ring vibrations. For pure hemin, signals at 628 and 587 cm^{-1} differ from the data at pD 1,⁴⁵ indicating the effect of SDS solvation and deprotonation of the heme propionates. In the data in the presence of imidazole, further ring vibrations arise, especially at 625 and 517 cm^{-1} ; the assignment to the ligand is confirmed by the shifts and signal splitting to 559 and 529 cm^{-1} due to isotope labeling. Free imidazole displays the ν_{25} mode, a coupled C4–C6 stretching and ring deformation at 657 cm^{-1} , and ν_{26} at 619 cm^{-1} , which is a ring torsion, C4–C6 wag motion.⁹ These modes shift to 559 and 529 cm^{-1} upon labeling. The signal at 625 cm^{-1} involves coordinates from the ring vibration of the imidazole ring.^{8,9,11,14,15}

The absorbance of hemin is dominated by the significant signal at 350 cm^{-1} , the Fe–OH stretching vibration. For hemin in the presence of imidazole (Figure 1C), this vibration is absent; the hydroxide molecule was exchanged by two imidazole ligands. Imidazole–iron–imidazole vibrations can now be observed at 396/386/378 cm^{-1} for hemin with imidazole and at 399/388/376 cm^{-1} for hemin with isotopic labeled imidazole. The signal at 386 and 317 cm^{-1} originates from the out-of-plane pyrrole tilting mode (pyr tilt) that would be expected around 350 cm^{-1} , however, this is split due to its coupling with the antisymmetric $\nu_{as}\text{FeIm}$. This was previously calculated and reported for a bis(imidazole)–Fe(III) (octaethylporphyrin) molecule.²³ The model used does not include the heme propionates and it has a fully symmetric porphyrin plane. We attribute the signal at 396 cm^{-1} , not observable in the model used by Mitchell et al.,²³ to this difference in symmetry. The Fe–Im vibrational frequency in the bis(imidazole)–iron protoporphyrin and in the bis(imidazole)–Fe(III) (octaethylporphyrin) molecule²³ is significantly higher than in high-spin five-coordinated monoidazole compounds.^{47–49} This difference can be related to the emptiness of the antibonding $d_z^2(\text{Fe})-\sigma(\text{NIm})$ σ orbital in the hexacoordinated compound studied here.⁴⁷

Temperature Dependence. Temperature-dependent measurements from 300 to 25 K have been performed in the spectral region from 650 to 100 cm^{-1} . In a first step, the effect of freezing on the spectral properties of the detergent has been monitored. A clear shift and splitting of the coupled CH_2 vibrations in the spectral range from 250 to 150 cm^{-1} , as displayed in Figure 2, can be reported. The peak at 212 cm^{-1} shifts about 16 cm^{-1} (to 228 cm^{-1}), increases in intensity, and loses half length width. Furthermore, a new signal at 174 cm^{-1} occurs. The appearance of relatively narrow peaks indicates the ordering of the SDS molecules, while the strong upward frequency shift of the liquid-phase band at 212 cm^{-1} suggests an increase in intermolecular connectivity. We conclude that crystallization should take place, at least partially, in our SDS sample between 200 and 100 K.

The absorbance spectra for hemin at 300, 200, 100, and 25 K are shown in Figure 3. Interestingly, the Fe–O(H) stretching vibration is not temperature-dependent. The signals at higher frequency increase slightly upon cooling. The strongest effect can be seen for the broad feature between 300 and 150 cm^{-1} . An upshift of 5 cm^{-1} can be observed for the ring vibration at 169 cm^{-1} (inset, Figure 3). The temperature-dependent signal increase is linear, as also found for coupled modes reported in crystals or frozen water.⁴⁰ The slight increase in the absorption in the 300–150 cm^{-1} range could be due to a larger number of hydrogen bonds being established. However, a crystal state seems not to be reached by hemin down to 25 K, since the absorption spectrum does not drastically change with temperature. The sudden shift of the ring vibration from 171 to

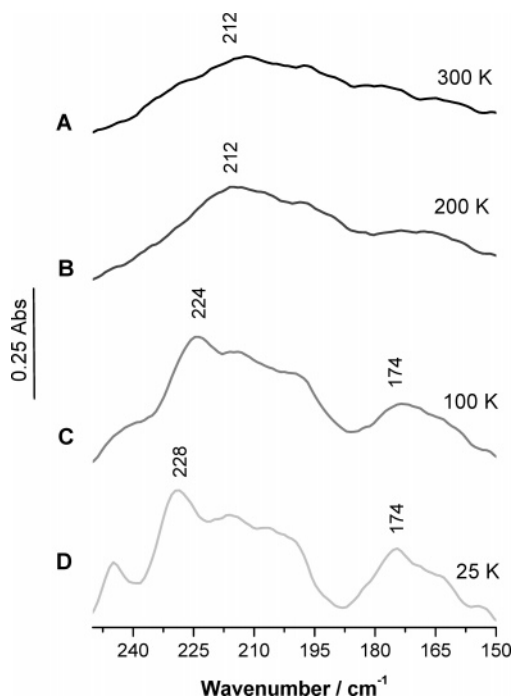


Figure 2. Absorbance data of SDS at (A) 300, (B) 200, (C) 100, and (D) 25 K.

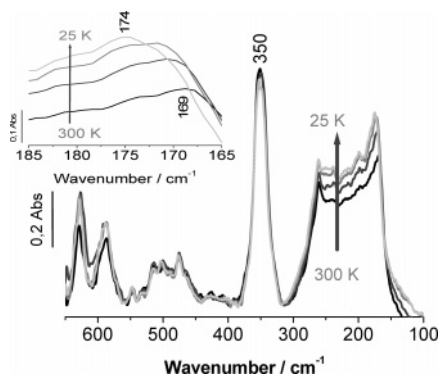


Figure 3. Absorbance data of hemin at 300–25 K between 650 and 100 cm^{-1} .

174 cm^{-1} upon cooling from 100 to 25 K suggests that crystallization may take place at lower temperatures, but a glassy behavior with no crystallization is also possible.

In a next step, the temperature dependent behavior of the bis(imidazole)–iron model was studied. Figure 4 displays the data between 420 and 360 cm^{-1} (A) and between 200 and 150 cm^{-1} (B) for several steps between 25 and 300 K. For the ring vibration at 172 cm^{-1} , also seen in the spectra of pure hemin (Figure 3), intensity increases upon cooling and an upshift to 178 cm^{-1} is evident. The shift differs slightly from the shift in the absence of the ligand, indicating some coupling.

The spectral range including the $\nu_{\text{as}}\text{FeImH} + \text{pyr tilt}$ vibration at 387 cm^{-1} reflects a linear increase of signal intensity and a shift toward higher wavenumbers. We note that the slope of the signal increase changes below 150 K, (see inset), possibly reflecting a temperature range where the molecule shows a structural transition. However, since no strong change of the spectral properties occurs, a full phase transition of the molecule does not seem likely. The clearest shift upon cooling is displayed by the signal at 396 cm^{-1} . Interestingly the mode at 377 cm^{-1} does not shift significantly, and a decrease in intensity and broadness is evident together with a different slope than for

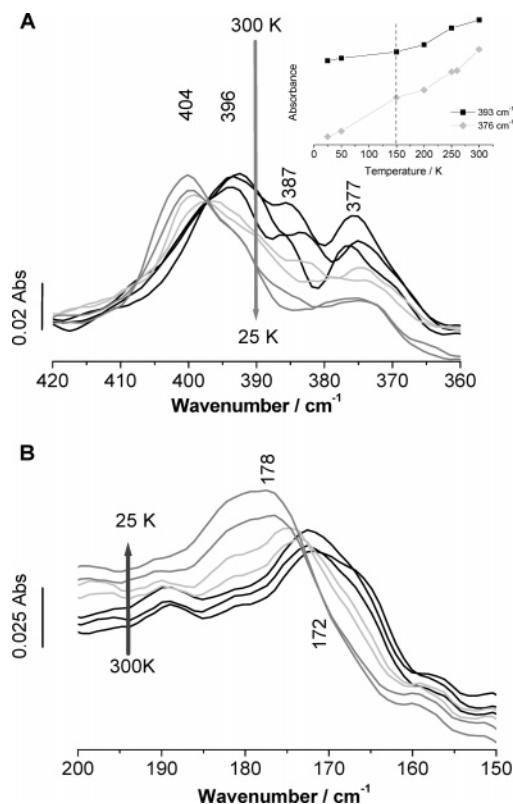


Figure 4. Temperature-dependent absorbance spectra of hemin with imidazole between 300 and 25 K in the spectral range from 420 to 360 cm^{-1} (A) and from 200 to 150 cm^{-1} (B).

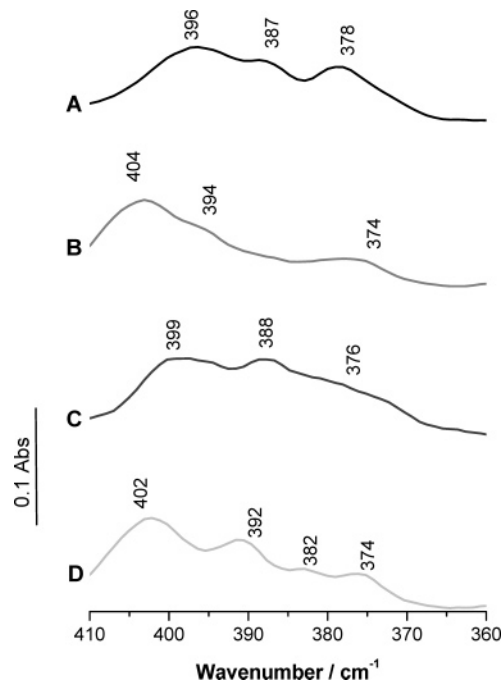


Figure 5. Comparison of the absorbance data of hemin with imidazole at (A) 300 and (B) 25 K and imidazole- d_4 at (C) 300 and (D) 30 K between 410 and 360 cm^{-1} .

the other features (see inset). This behavior is typical for motions with bending character.⁴⁶

Most interestingly, the broad feature between 410 and 370 cm^{-1} for the d_4 -labeled and nonlabeled imidazole-bound hemin shows a distinct temperature-dependent behavior. Figure 5 shows the comparison of the absorbance data of hemin–imidazole at 300 K (A)/25 K (B) and of hemin with isotopic

labeled imidazole- d_4 at 300 K (C)/30 K (D). At 300 K, three signals are observable: namely, for imidazole at 396/386/378 cm^{-1} and for imidazole- d_4 at 399/388/376 cm^{-1} . The shape, however, indicates that a fourth feature may be hidden. Upon cooling, the signals at 396 and 386 cm^{-1} shift 7/6 cm^{-1} to 404 and 394 cm^{-1} and after isotope labeling from 399 and 392 cm^{-1} shift 3 cm^{-1} to 402, 392, and 382 cm^{-1} . The signal at 378 cm^{-1} shifts to 374 cm^{-1} and decreases. This mode does not seem to be sensitive to isotope labeling and the motion freezes at low temperatures. A possible explanation for these complex shifts includes the possibility that the broad feature is composed by a number of bands, superimposing a clear shift of the $\nu_{\text{as}}\text{FeImH} + \text{pyr tilt}$. Alternatively it might be assumed that the couplings of the modes, or anharmonicity effects, are suppressed at low temperatures.

Conclusions

In this study we present the first infrared spectroscopic evidence for the Fe–Im vibration in far-infrared of a heme B analogue compound: bis(imidazole)–iron protoporphyrin. The molecule is studied in SDS solution in order to mimic the hydrophobic environment of a protein.

The imidazole–iron–imidazole vibration can be observed at 396/386/378/317 cm^{-1} for hemin with imidazole and clearly changes upon d_4 labeling of the imidazol ligands to 399/388/376/313 cm^{-1} . The signal at 386 and 317 cm^{-1} originates from the out-of-plane pyrrole tilting mode (pyr tilt) coupled with the antisymmetric $\nu_{\text{as}}\text{FeIm}$. An earlier study by the Spiro group presented a more symmetric model compound, where the heme propionates were absent.²³ Correspondingly, a more complex spectrum can be reported here, including the signals at 396 and 387 cm^{-1} .

The position observed for the Fe–Im vibrational frequency is higher than in previously reported high-spin five-coordinated monoimidazole compounds.^{47–49} Stravrov⁴⁷ previously demonstrated the influence of the sixth ligand and related the shift in frequency to the emptiness of the antibonding d_z^2 (Fe)– $p\sigma(\text{NIm})$ σ orbital.

Temperature-dependent spectroscopy was utilized to learn more about these vibrations, for its sensitivity to anharmonic couplings and to differentiate the different motions. The low-temperature form of the ring should be of higher symmetry and with stronger bonds. Upon cooling from 300 to 25 K, the peak at 387 cm^{-1} disappears, and the peaks at 396 and 172 cm^{-1} shift by 10 cm^{-1} . Clearly a transition is seen at 150 K. However, the absorption spectrum does not drastically change with temperature, and a crystal state seems not to be reached by hemin or by the ligand-bound form down to 25 K. The sudden shift of the ring vibration from 171 to 174 cm^{-1} upon cooling from 100 to 25 K suggests that crystallization may take place at lower temperatures, but a glassy behavior with no crystallization is also possible. This spectral feature, which is not isotope-sensitive, changes the slope of the frequency shift in the imidazole-bound form, due to the influence of the temperature on coupled motions.

Future studies will involve theoretical calculations of the temperature-dependent motions of these molecules and the experimental approach toward proteins.

Acknowledgment. We thank the Deutsche Forschungsgemeinschaft (DFG, SFB 472), the BMBF (05 ES3XBA/5), and the Université Louis Pasteur, Strasbourg, for financial support.

References and Notes

- Perutz, M. F. *Br. Med. Bull.* **1976**, 32 (3), 195–208.
- Adman, E. T. *Adv. Protein Chem.* **1991**, 42, 145–197.
- Regan, L. *Annu. Rev. Biophys. Biomol. Struct.* **1993**, 22, 257–287.
- Isaac, I. S.; Dawson, J. H. *Essays Biochem.* **1999**, 34, 51–69.
- McCall, K. A.; Huang, C.; Fierke, C. A. *J. Nutr.* **2000**, 130 (55), 1437S–1446S.
- Kerr, E. A.; Yu, N.-T.; Gersonde, K.; Parish, D. W.; Smith, K. M. *J. Biol. Chem.* **1985**, 260 (23), 12665–12669.
- Sawai, H.; Makino, M.; Mizutani, Y.; Ohta, T.; Sugimoto, H.; Uno, T.; Kawada, N.; Yoshizato, K.; Kitagawa, T.; Shiro, Y. *Biochemistry* **2005**, 44, 13257–13265.
- Hasegawa, K.; Ono, T.-A.; Takumi, N. *J. Phys. Chem. B* **2000**, 104, 4253–4265.
- Hasegawa, K.; Ono, T.-A.; Noguchi, T. *J. Phys. Chem. A* **2002**, 106, 3377–3390.
- Muehlinghaus, J.; Zundel, G. *Biopolymers*, **1971**, 10 (4), 711–719.
- Venjaminov, S. Y.; Kalnin, N. N. *Biopolymers* **1990**, 30, 141–173.
- Barth, A. *Prog. Biophys. Mol. Biol.* **2000**, 74, 141–173.
- Mesu, J. G.; Visser, T.; Soulimani, F.; Weckhuysen, B. M. *Vib. Spectrosc.* **2005**, 39, 114–125.
- Matei, A.; Drichko, N.; Gompf, B.; Dressel, M. *J. Chem. Phys.* **2005**, 121, 61–71.
- Wolpert, M.; Hellwig, P. *Spectrochim. Acta* **2006**, 64, 987–1001.
- Berthomieu, C.; Boussac, A. *Biochemistry* **1995**, 34, 1541–1548.
- Noguchi, T.; Inoue, Y.; Tang, X.-S. *Biochemistry* **1999**, 38, 399–403.
- Noguchi, T.; Inoue, Y.; Tang, X.-S. *Biochemistry* **1999**, 38, 10187–10195.
- Hiser, C.; Mills, D. A.; Schall, M.; Ferguson-Miller, S. *Biochemistry* **2001**, 40, 1606–1615.
- Tomson, F.; Bailey, J. A.; Gennis, R. B.; Unkefer, J. U.; Li, Z.; Silks, L. A.; Martinez, R. A.; Donohoe, R. J.; Dyer, R. B.; Woodruff, W. H. *Biochemistry* **2002**, 41, 14383–14390.
- Iwaki, M.; Yakovlev, G.; Hirst, J.; Osyczka, A.; Dutton, P. L.; Marshall, D.; Rich, P. R. *Biochemistry* **2005**, 44, 4230–4237.
- Iwaki, M.; Puustinen, A.; Wikström, M.; Rich, P. R. *Biochemistry* **2006**, 45, 10873–10885.
- Mitchell, M. L.; Li, X.-Y.; Kincaid, J. R.; Spiro, T. G. *J. Phys. Chem.* **1987**, 91, 4690–4696.
- Argade, P. V.; Sassaroli, M.; Rousseau, D. L.; Inubushi, T.; Ikeda-Saito, M.; Lapidot, A. *J. Am. Chem. Soc.* **1984**, 106, 6593–6596.
- Nagai, K.; Kitagawa, T.; Morimoto, H. *J. Mol. Biol.* **1980**, 136, 271–289.
- Scott, T. W.; Friedman, J. M. *J. Am. Chem. Soc.* **1984**, 106, 5677–5687.
- Sage, J. T.; Morikis, D.; Champion, P. M. *Biochemistry* **1991**, 30, 1227–1237.
- Woodruff, W. H.; Einarsdottir, O.; Dyer, R. B.; Bagley, K. A.; Palmer, G.; Atherton, S. J.; Goldbeck, R. A.; Dawes, T. D.; Klier, D. S. *Proc. Natl. Acad. Sci.* **1991**, 88, 2588–2592.
- Choi, S.; Spiro, T. G. *J. Am. Chem. Soc.* **1983**, 105, 3683–3692.
- Choi, S.; Lee, J. J.; Wei, Y. H.; Spiro, T. G. *J. Am. Chem. Soc.* **1983**, 105, 3692–3707.
- Carter, D. A.; Pemerton, J. E. *J. Raman. Spectrosc.* **1997**, 28, 939–946.
- Boffi, A.; Kanti Das, T.; della Longa, S.; Spagnuolo, C.; Rousseau, D. L. *Biophys. J.* **1999**, 77, 1143–1149.
- Bitler, A.; Stavrov, S. S. *Biophys. J.* **1999**, 77, 2764–2776.
- Franzen, S.; Fritsch, K.; Brewer, S. H. *J. Phys. Chem. B* **2002**, 106, 11641–11646.
- Loapro, J. J.; Cheatum, C. M.; Ondrias, M. R.; Simpson, M. C. *J. Chem. Phys.* **2003**, 119, 353–374.
- Cupane, A.; Leone, M.; Unger, E.; Lemke, C.; Beck, M.; Dreybrodt, W.; Schweitzer-Stenner, R. *J. Phys. Chem. B* **1998**, 102, 6612–6620.
- Li, J.; Lee, S. A.; Anderson, A.; Lettress, L.; Griffey, R. H.; Mohan, V. *J. Raman Spectrosc.* **2003**, 34, 183–191.
- Whitmire, S. E.; Wolpert, D.; Markelz, A. G.; Hillebrecht, J. R.; Galan, J.; Birge, R. R. *Biophys. J.* **2003**, 85 (2), 1269–1277.
- Zelmsmann, H. R. *J. Mol. Struct.* **1995**, 350, 95–114.
- Brubach, J.-B.; Mermet, A.; Filabozzi, A.; Gerschel, A.; Roy, P. *J. Chem. Phys.* **2005**, 122, 184509.
- Cannon, J. B.; Kuo, F. S.; Pasternack, R. F.; Wong, N. M.; Muller-Eberhard, U. *Biochemistry* **1984**, 23 (16), 3715–3721.
- Collins, D. M.; Countryman, R.; Hoard, J. L. *J. Am. Chem. Soc.* **1972**, 94, 2066–2067.
- Hunt, N. T.; Turner, A. R.; Wynne, K. *J. Phys. Chem. B* **2005**, 109 (4), 19008–19017.
- Klug, D. D.; Zgierski, M. Z.; Tse, J. S.; Liu, Z.; Kincaid, J. R.; Czarnecki, K.; Hemley, R. J. *Proc. Natl. Acad. Sci. U.S.A.* **2002**, 99, 12526–12530.

- (45) Dörr, S.; Schade, U.; Hellwig, P.; Ortolani, M. (submitted for publication).
- (46) Matei, A. Optical Investigations of Biological Samples in Far Infrared. Dissertation, University of Stuttgart, Germany, 2005.
- (47) Stravrov, S. S. *Biophys. J.* **1993**, 65, 1942–1950.
- (48) Kitagawa, T. The heme protein structure and the iron histidine

stretching mode. In *Biological Applications of Raman Spectroscopy*; Spiro, T. G., Ed.; Wiley and Sons: New York, 1988; Vol. III, pp 97–131.

- (49) Rousseau, D. L.; Friedman, J. M. Transient and cryogenic studies of photodissociated haemoglobin and myoglobin. In *Biological Applications of Raman Spectroscopy*; Spiro, T. G., Ed.; Wiley and Sons: New York, 1988; Vol. III, pp 133–215.